INTERNATIONAL ATOMIC ENERGY AGENCY
UNITED NATIONS EDUCATIONAL, SCIENTIFIC AND CULTURAL ORGANIZATION
INTERNATIONAL CENTRE FOR THEORETICAL PHYSICS
I.C.T.P., P.O. BOX 586, 34100 TRIESTE, ITALY, CABLE CENTRATOM TRIESTE

IN REPLY PLEASE REFER TO

SMR.380/24

COLLEGE ON THEORETICAL AND EXPERIMENTAL RADIOPROPAGATION SCIENCE

6 24 February 1989

THE CONCEPTS AND PRACTICE OF IONOSPHERIC PROPAGATION PREDICTIONS

B.M. REDDY

National Physical Laboratory
New Delhi 110012

These notes are intended for internal distribution only.

THE CONCEPTS AND PRACTICE OF IONOSPHERIC PROPAGATION PREDICTIONS

B.M. Reddy and S. Aggarwal
National Physical Laboratory
New Delhi-110012, India

1. Introduction:

The ionosphere is produced essentially by the solar EUV and X-rays at all latitudes and to some extent by the solar particles at high latitudes. The F-layer is the most important region for long distance HF communications though E-layer is also used for shorter distances during daytime. The D-region is a nuisance for HF communications as it absorbs radio wave energy during day-lit hours. D-region can also be used for some specialised services in the LF and VLF bands and also in the VHF band through scatter mechanisms; but any further discussion on these topics is beyond the scope of this presentation. It is known for quite some time now that the solar ionising radiations in the EUV and X-ray regions display a distinct 11-year cycle, similar to the sunspot cycle. It should be added here that the total energy in the EUV and X-ray regions is but an insignificant part of the total solar radiant energy; but it is enough to produce and maintain the ionosphere in the tenuous reaches of our upper atmosphere. For the very reason that EUV and X-rays produce the ionosphere, they do not reach the earth and hence cannot be monitored through ground-based experiments. One is thus compelled to look for a surrogate index that correlates with the ionising radiations, but can be monitored from the earth. One such index with a long series of observations is the Sun-Spot Number (SSN). Fig. 1 shows the 12-month running average Sun-Spot Number and the noon f_oF_2 values for Kodaikanal in the bottom and top panels respectively for the period 1954-83. The trend of the $f_o F_2$ values very closely follows the Sun-Spot Number as is obvious from the figure and the seasonal variations superposed on the solar activity variations are

also obvious.

It is also educative to study the local time variations of the critical frequencies of the different layers at solar minimum and maximum. Figure 2 shows these variations for an equatorial station, Kodaikanal while Fig. 3 shows the same variations for Ahmedabad which is near the equatorial anomaly peak. The salient features that are obvious may be summarised as follows:

The predominance of the sporadic-E layer very often exceeding the F_2 layer electron densities is obvious at Kodaikanal. Also the F_2 layer critical frequencies are lower at Kodaikanal compared to Ahmedabad because of the equatorial anomaly. The winter anomaly is obvious from Fig. 3 for Ahmedabad, where during solar maximum the F_2 critical frequencies are much higher during winter than during summer. The very large changes during dawn are remarkable both at Kodaikanal and at Ahmedabad in the F_2 layer critical frequencies which incidentally pose serious problems in communications during the morning hours. Also spectacular is the continued high level of ionisation in the F_2 layer even after sun-set at Ahmedabad during the winter of solar maximum, which unerlines the importance of winds and other transport processes. In fact, the mid-night electron densities remain almost as high as the noon densities most of the time.

As the ionospheric data accumulated over the years and the ground-based solar observations were diversified with systematic observations of solar radio flux, search was on for indices that reflect the ionospheric response better. In addition to better correlation, the index should be predictable with some confidence. It is here that

R_{12}, the 12-month running mean sun-spot number, scores due to the lognest series of available observations. It, however, is of little use to predict short-term variability. The systematic observations of solar radio flux (Ø) around a wavelength of 10 cm in Cananda, Japan and elsewhere are made since 1947. Very good linear relationships are found between R_{12} and $Ø_{12}$ (Stewart and Leftin, 1972). The ionospherically derived index IG (Liu et al 1983) did show some improvement at least for mid latitudes; another ionosphere-based index IF_2 , based on noon f_oF_2 values also showed good correspondence with f_oF_2 (Minnis, 1964). But these indices are not universal and prove to be good only for those regions that gave the ionospheric data input in deriving them. An attempt has been made recently (Lakshmi et al 1988) to use the satellite measurements of EUV radiations (1977-1980) to predict ionospheric parameters; but the available data perhaps is yet inadequate to develop a formal index.

2. Data Acquisition, Status and Preparation of Prediction Charts

2.1 Data Acquisition and Status

The data for producing the radio propagation predictions have been obtained by vertical incidence souding of the ionosphere. These soundings have been made at an interval of one hour, at least, over many years (since Dec. 1929 at Fort Belvoir, Washington in USA and since Jan. 1930 at Slough UK) at a number of places throughout the world. In addition to providing data for radio propagation predictions these data are used for research into the behaviour of the ionosphere. A system of International exchange of ionospheric data has been operating for many years. National Physical Laboratory at New Delhi holds a great deal of data from other parts of the world in addition to the Indian Data. Fig. 4 shows the network of all ionosphere sounding

stations known to have existed from time to time. Some of the stations operated only during certain special observational programmes like IGY, IQSY, IASY etc. All the basic parameters that are scaled and published in ionospheric data bulletins, are shown in Table 1.

TABLE 1

Important Parameters scaled

1. Frequencies	:	$f_oF_2, f_oF_1, f_oE, f_oE_s, f_bE_s$ and f_{min}
2. Minimum Virtual Heights	:	$h'F_2$, h'F, h'E, $h'E_s$
3. MUF factors	:	$M(3000)F_2$, $M(3000)F_1$
4. E_s types	:	f,l,c,h,q,r,a,s,d,n,k

Most of the published and unpublished data is held at four World Data Centres (WDC) viz. WDC at Boulder, USA, WDC at United Kingdom, WDC at MOSCOW, USSR and WDC at Tokyo, Japan. At NPL, we have the associated Regional Warning Centre under the IUWDS and all the published data is received through International Exchange system in exchange to the Ionospheric Data for Indian Stations (Table 1) published from NPL, New Delhi. Data from most of the stations is available within two years of its acquisition.

2.2 Ionospheric Propagation Predictions

Ionosphere affects the propagation of radio waves in two ways: advantageously by enabling communication (e.g. reflection) and adversly by scattering, absorbing, producing multipath etc. that interefere with optimum traffic requirements. It is divided into three regions or layers designated D, E and F respectively, in order of increasing altitude. Sub-division of these layers may exist under

layers act principally as radiowave relectors and permit long range propagation between terrestrial terminals. The D region acts principally as an absorber, causing signal attenuation in the HF range (3-30 MHz). VHF signals used in space communication are modified and degraded to varying degrees in passing through the ionosphere.

Ionospheric Predictions signify the process of foretelling the state of the ionosphere for a specified point in time and space and its effects on the operability of communication circuit i.e. mode availabilities and reliabilities of frequencies in HF band for ionospheric support. The longterm correspondence between sunspot numbers and noontime monthly median $f_o F_2$ at Kodaikanal, has been shown in Fig. 1.

While considering the predictions of monthly median ionospheric propagation conditions, it is essential to consider separately the translation of vertical incidence ionospheric data into oblique incidence characteristics and the prediction of vertical incidence data which is dependent on the accuracy and availability of ionospheric observations as well as predictions of other geophysical phenomena.

Thus, prediction of ionospheric data requires an accurate and reliable representation (either graphical or mathematical) and a known correlation with solar activity.

When ionospheric observation stations were less and fast computing devices were not available most of the ionospheric data

was represented graphically like the ones shown in Fig. 5. over limited longitude zones (within which variations were considered negligible if local time features were retained). With more and more vertical incidence stations being commissioned it became possible to map these characteristics on world maps showing longitudinal and latitudinal behaviours for fixed universal time. The seasonal variations were and are still incorporated using separate maps for separate months. CCIR Atlas of ionospheric characteristics (Report 340) gives world maps for two fixed solar activity levels 0 and 100. With the advent of computers sophisticated mathematical techniques have been applied to represent the vertical incidence ionospheric observations and the representations are also available in the form of numerical coefficients for use in computer programme. For numerical mapping of any ionospheric characteristic, say $\mathcal{N}$, considered to be a function of latitude, longitude and time i.e. $\mathcal{N}(\lambda, \theta, T)$ represents the value of a characteristic at a location (λ, θ) at time T, λ can take values from -90° to +90° of latitude, θ can be -180° to + 180° of longitude and T is 24 hours of a day.

$$\mathcal{N}(\lambda,\theta,T) = a_0(\lambda,\theta) + \sum_{j=1}^{H} \left[a_j(\lambda,\theta)\cos jT + b_j(\lambda,\theta)\sin jT \right]$$

H being the number of harmonics representing time variation and where

$$\left.\begin{aligned} a_j(\lambda,\theta) &= \sum_{k=0}^{K} U_{2j,k}\, G_k(\lambda,\theta) \\ \text{and } b_j(\lambda,\theta) &= \sum_{k=0}^{K} U_{2j-1,k}\, G_k(\lambda,\theta) \end{aligned}\right\} j = 0, 1, 2 \cdots H$$

give the latitudinal and longitudinal variations of the coefficients

$$a_j(\lambda,\theta) \quad \text{and} \quad b_j(\lambda,\theta)$$

Table 3 shows a set of geographic functions $G_k(\lambda,\theta)$: Here, q_i $(i = 0, 1, ---, m)$ denotes the highest power of Sin X for the i^{th} order harmonic in longitude and m may change from one ionospheric characteristic to another. However, the general form of the numerical maps will remain fixed. For indexing purposes it is sometimes convenient to introduce the sequence k_i, $(i = 0, 1, \ldots, m)$ such that $G_k(\lambda,\theta)$ is the last of the geographic functions of i^{th} order longitude:

$$G_{k_o}(\lambda,\theta) = \text{Sin}^{q_o}\chi$$

$$G_{k_i}(\lambda,\theta) = \text{Sin}^{q_i}\chi \cos^{i}\lambda \text{ Sin } i\theta$$

Thus

$$q_o = k_o \; ; \quad q = \frac{k_i - k_{i-1}}{2}, \quad i = 1\ 2, --m$$

and the total number of geographic function in Table 3 is given by

$$K + 1 = k_m + 1$$

and

$$\text{Sin } X = \sqrt{\frac{I}{(I^2 + \text{Cos}\lambda)}}$$

where I is the magnetic dip.

Now the procedure described by Jones and Gallet (1962) may be used to obtain the coefficients $U_{s,k}$ for defining $a_j(\lambda,\theta)$ and $b_j(\lambda,\theta)$ in Eqn. (1).

2.3 Predicting Effect of F-region Ionoization on Radio Communications

Long term ionospheric prediction of basic F2-layer MUF i.e. of f_oF_2 and MUF (4000) F2 have been prepared and printed in the form of an Atlas (CCIR Report 340). CCIR gives graphical contour maps for two levels of solar activity viz 0 and 100 and for other levels of solar activity linear interpolation or extrapolation is performed. The CCIR values are also available in computer routine.

Institute of Telecommunication Sciences at Boulder had prepared similar world maps for three levels of solar activity (Sunspot Numbers = 10, 110, 160) where linear interpolation is affected between any two parts depending if SSN lies between 10 and 110 or between 110 and 160.

2.4 Prediction Procedure at RSD

The critical frequency and maximum usable frequency for a distance of 4000 km for the East zone (50°E - 170°E) are provided in the form of contour maps for fixed frequencies on latitude vs. local time scale, six months in advance since fifties. The basis of these predictions (Fig.5) are the ionosonde data for forty stations within the zone (Table 4). Predicted values of sunspot number are used to obtain the critical frequencies and height factors which show very good statistical relationship with sunspot numbers. In the beginning, linear relations were obtained, which failed after the data near the peak of nineteenth cycle (for SSN $\simeq$ 150) were added and foF2 showed saturation effect for higher sunspot range. Most of the calculations were carried out manually with the help of graphs and nomograms. Now we have on

an average more than 40 years of data per station. Most of which has been transferred to magnetic tape for computer use and 2nd degree curves are fitted every hour with the help of computer. Fig. 6 shows a comparison of the observed and predicted values for Delhi.

Once all the coefficient A,B,C of second degree curve:

$$F(x) = A + BR_{12} + CR_{12}^2 \qquad .. (2)$$

where F(x) is either foF2 or M(3000) F2 at a particular hours, are obtained, predictions for each month can be presented at contour maps of the constant A,B,C in latitude vs. local time and for all the twelve months. These would form the prediction charts on almost permanent basis. These coefficients can be revised every five years. A sample contour map for January over the Indian continent is shown in Fig.7. Similar maps will be available either of M(4000) F2 or for MUF (4000) F2. Once a sunspot No.R12 is predicted using the relation (2) and reading A,B,C from the map will give the required predicted value of the frequency.

For use on a computer the constants can be supplied as arrays on computer cards with appropriate programmes and with a very small number of input parameters like location of the terminals and predicted sunspot number circuit predictions can be obtained.

2.5 Predicting the effect of F1 layer on radiowave communication

An F1-layer prediction system has been developed in the range 2000 to 3400 km. foF1 can be determined for any value of R12 from the following expressions (Ducharme, Petrie and Eyfrig, 1973).

$$foF1 = f \quad \cos^n \chi$$

where

$$f_s = f_{so} + 0.01\ (f_{s100} - f_{so})\ R_{12}$$

$$f_{so} = 4.35 + 0.0058\,\lambda - 0.000120\,\lambda^2$$

$$f_{s100} = 5.35 + 0.0110 - 0.00230\,\lambda^2$$

$$n = 0.093 + 0.00461\,\lambda - 0.0000540\,\lambda^2 + 0.00031\,R_{12}$$

The maximum solar zenith angle χ at which F1 layer is present is given by the following:

$$\chi_m = \chi_0 + 0.01\ (\chi_{100} - \chi_0) R_{12} \quad \text{(degrees)}$$

where

$$\chi_0 = 50 + 3.48\,\lambda$$

$$\chi_{100} = 38.7 + 0.509\,\lambda$$

For oblique frequency of transmission the factor J is given as:

$$J \text{ factor} = J_0 - 0.01\ (J_0 - J_{100})\ R_{12}$$

$$J_0 = 0.16 + 2.64 \times 10^{-3} D - 0.40 \times 10^{-6} D^2$$

$$J_{100} = -0.52 + 2.69 \times 10^{-3} D - 0.39 \times 10^{-6} D^2$$

where D represents the great circle distance in kilometers in the range 2000 to 3400 km. The F1-layer MUF is computed by multiplying the foF1 by the J factor.

2.6 Predicting the Efffects of E-region Ionization on Radiowave Communications

The effect of regular E-layer on propagation can be determined from a series of empirical formulae given below (Muggleton,1975)

$$(foE)^4 = A.B.C.D.$$

where A,B,C,D involve solar activity, season, geographic position and time respectively and are described as below:

The solar activity function, A

$$A \approx 1 + 0.0091R$$

or $$A = 1 + 0.0094 \cdot (\phi - 66)$$

or $$A = (1 + 0.00144\ IF2)^4$$

where R and IF2 are in sunspot units and the unit of ϕ is 10^{-22} Wm^{-2} Hz^{-1}.

The season function, B

$$B = (\cos\chi_{noon})^m$$

$$m = -1.93 + 1.92 \cos\lambda \text{ for } |\lambda| < 32°$$

$$= 0.11 - 0.49 \cos\lambda \text{ for } |\lambda| \gtrsim 32°$$

λ being the geographic latitude

The position function, C

$$C = X + Y \cos\lambda$$

where $X = 23,\ Y = 116$ for $|\lambda| < 32°$

and $X = 92,\ Y = 35$ for $|\lambda| \gtrsim 32°$

The time-of-day function, D

$$D = (\cos\chi)^P$$

where $P = 1.20$ for $|\lambda| > 12°$

and $= 1.31$ for $|\lambda| \leq 12°$

For small values of and to incorporate larger values

$$D = [\cos(\chi - \delta\chi)]^P \quad \text{for } 70° \leq \chi \leq 90°$$

with $\delta\chi = 6.27 \times 10^{-13} [\chi - 50]^{8.02}$ and

P defined as above

The nighttime model then becomes

$$D = (0.077)^P \exp.\ [-1.68\ (T_1 - t)] \text{ for } |\chi| > 90°$$

from midnight to dawn

or $D = (0.077)^P \exp.\ [-1.01\ (t - T2)$ from sunset to midnight

The effects of sporadic E are not well unerstood because of the highly variable nature of the occurrence and intensity of sporadic E ionization and prediction systems are based on statistics. Numerical maps for the worldwide occurrences of sporadic E for minimum and maximum solar activity and the blanketing sporadic E for a year of minimum solar activity are available. It is possible to calculate the fraction of time sporadic E can support HF or VHF communication or interfere with regular HF communication.

All these are required to predict the average state of the ionosphere but for HF to be operational another factor that is very essential is the percent of the days ionospheric support will be available to a particular frequency. For this statistical distribution function of day-to-day values around the median are required. For parabolic layer theory and assuming a normal distribution around the median 0.85 times the median frequency, a frequency exceeded 90% of the times, is defined as optimum working frequency (OWF).

But as more and more data is becoming available it is possible with the help of computers to get the exact distribution functions and different percentiles. The lower deciles in this case is found to be different for different times of the day and station and level of solar activity. Fig. 8 shows a sample calculation for

Kodaikanal, winter low solar activity. Bradley (1976) has fitted two separate normal function to values above and values below the median and obtained the following empirical relations for circuit availability, Q :

$$\text{for} \quad f \leq f_m$$

$$Q' = 130 - \frac{80}{1 + \dfrac{1 - f/f_m}{1 - F_l}} \quad \text{or } 100, \text{ (whichever is smaller)}$$

and for $f \geq f_m$

$$Q = \frac{80}{1 + \dfrac{f/f_m - 1}{F_u - 1}} - 30 \text{ or } 0 \quad \text{(whichever is larger)}$$

for F region support where f is the frequency of operation F_u , F_l are ratios of upper decile and lower decile to the median MUF respectively.

The other regions do not show large variability and so are quite well defined by the equations discussed earlier.

The final reliability of a circuit is a combination of the mode availability and the availability of a signal to noise ratio above a certain threshold which in turn depends on the radiated power and a number of propagation losses.

REFERENCES

Aggarwal, S., Day-to-day Variability in foF2 at low latitudes over a solar cycle, Indian J. Radio and Space Phys., 14, 73, 1985.

CCIR Atlas of Ionospheric Characteristics, Report 340, International Telecommunication Union, Geneva 1983.

Ducharme, E.D., L.E. Petrie and R. Eyfrig., A method for predicting the F1-layer critical frequency based on the Zurich smoothed sunspot number., Radio Sci., 8, (New series), 837, 1973.

IPSD (1968). The development of ionospheric index T, Report IPS-R11 Ionospheric prediction service, Sydney, Australia.

Joachim, M., Study of correlation of three basic indices of ionospheric propagation, R12, IF2 and Ø, Nature, 210, 289, 1966.

Joachim, M. and Y. Krupin, Correlation entre les indices R12 et Ø12 relatifs a'la propagation ionospherique, C.R. Acad. Sci. (Paris) B, 269, 664, 1969.

Jones, W.B. and R.M. Gallet., Representation of diurnal and geographic variations of ionospheric data by numerical methods, ITU Telecommunication Journal, 29, 129, 1962a.

Jones, W.B. and R.M. Gallet, Methods for applying numerical maps of ionospheric characteristics, Journal of Resarch NBS, 66D(6) 649, 1962b.

King J.W. and A.J. Slater, Errors in predicted values of foF2 and hmF2 compared with day-to-day variability, ITU Telecommunication Journal, 40, 766, 1973.

Lakshmi, D.R., Reddy, B.M. and Dabas, R.S., On the possible use of recent, EUV data for ionospheric preeictions, J. Atmosph. Terr. Phys., 50, 207, 1988.

Leftin, M., Numerical representation of monthly median critical frequencies of the regular E-region (foE), Office of Telecommunication Rpt. 76-78. Suptt. of Documents US Printing Office, 1976.

Liu, R.Y., P.A. Smith and J.W. King, A new solar index which leads to improved foF2 predictions using the CCIR Atlas. Telecommunications Journal, 50, 408, 1983.

Minnis, C.M., Ionospheric Indices (a review), Advances in Radio Research, 2,1964.

Muggleton, L.M., A method of predicting foE at any time and place. Telecomm. J. 42, 413, 1975.

Reddy, B.M., S. Aggarwal, D.R. Lakshmi, S. Shastri and A.P. Mitra, Longterm solar activity and ionospheric prediction services rendered by the National Physical Laboratory, New Delhi, Solar Terr.Predictions Proc. 1, 118, 1979.

Stewart, F.G. and M. Leftin, Relations between Ottawa 10.7 cm solar noise flux and Zurich sunspot number. Telecomm. Jour. 39, 159, 1972.

TABLE 2

INDIAN IONOSPHERIC STATIONS

Station	Latitude Geographic	Longitude Geographic	Latitude Geomagnetic	Latitude Magnetic (°)	Magnetic Dip (°)
Delhi	28°38'N	77°13'E	19°11'N	24.8 N	42.44 N
Ahmedabad	23°01'N	72°36'E	14°01'N	18.6 N	34.0 N
Haringhata (C alcutta)	22°58'N	88°34'E	12°15'N	17.5 N	32.0 N
Bombay	19°00'N	72°50'E	10°00'N	13.0 N	24.75NN
Hyderabad	17°21'N	78°28'E	7°39'N	11.1 N	21.5 N
Madras	13°05'N	80°17'E	3°05'N	5.3 N	10.5 N
Tiruchirapalli	10°49'N	78°42'E	1°05'N	2.4 N	4.8 N
Kodaikanal	10°14'N	77°29'E	0°44'N	1.75N	3.5 N
Thumba (Trivandrum)	8°33'N	76°52'E	0°38'S	0.3 N	0.6 S

TABLE 3

GEOGRAPHIC COORDINATE FUNCTIONS G_k (λ, θ)

(X is a function of λ and θ, m is the maximum order in longitude)

k	Main latitude variation	k	First order longitude, G_k	k	Second order longitude, G_k	...	k	mth order longitude
0	1	$k_0 + 1$	$\cos\lambda\ \cos\theta$	$k_1 + 1$	$\cos^2\lambda\ \cos\ 2\theta$	...	$k_{m-1} - 1$	$\cos^m\lambda\ \cos m\theta$
1	$\sin\ X$	$k_0 + 2$	$\cos\lambda\ \sin\theta$	$k_1 + 2$	$\cos^2\lambda\ \sin\ 2\theta$	...	$k_{m-1} + 2$	$\cos^m\lambda\ \sin m\theta$
2	$\sin^2\ X$	$k_0 + 3$	$\sin X\ \cos\lambda\ \cos\theta$	$k_1 + 3$	$\sin X\ \cos^2\lambda\ \cos\ 2\theta$	...	$k_{m-1} + 3$	$\sin X\ \cos^m\lambda\ \cos m\theta$
.		$k_0 + 4$	$\sin X\ \cos\lambda\ \sin\theta$	$k_1 + 4$	$\sin X\ \cos^2\lambda\ \sin\ 2\theta$	...	$k_{m-1} - 4$	$\sin X\ \cos^m\lambda\ \sin m\theta$
. . .		. . .		. . .			. . .	
k_0	$\sin^{q_0}\ X$	$k_1 - 1$	$\sin^{q_1}\ X\ \cos\lambda\ \cos\theta$	$k_2 - 1$	$\sin^{q_2}\ X\ \cos^2\lambda\ \cos\ 2\theta$	...	$k_m - 1$	$\sin^{q_m} X\ \cos^m\lambda\ \cos m\theta$
.		k_1	$\sin^{q_1}\ X\ \cos\lambda\ \sin\theta$	k_2	$\sin^{q_2}\ X\ \cos^2\lambda\ \sin\ 2\theta$	...	k_m	$\sin^{q_m} X\ \cos^m\lambda\ \sin m\theta$

TABLE 4

LIST OF STATIONS USED IN IONOSPHERIC PREDICTIONS

AT

NATIONAL PHYSICAL LABORATORY, NEW DELHI

Code	Name	Latitude	Longitude
01	Clyde	70.5	-68.60
02	Wakkanai	45.45	141.69
03	Akita	39.37	140.13
04	Tokyo (Kokubunji)	35.71	139.48
05	Yamagawa	31.20	130.61
06	Delhi	28.60	77.20
07	Okinawa	26.28	127.81
08	Formosa (Taipei)	24.91	121.24
09	Ahmedabad	23.00	72.60
10	Haringhata (Calcutta)	23.00	88.60
11	Bombay	19.00	72.80
12	Baguio	16.40	120.60
13	Madras	13.10	80.30
14	Tiruchirapalli	10.80	78.70
15	Kodaikanal	10.20	77.50
16	Singapore	1.30	103.80
17	Townsville	-19.63	146.85
18	Brisbane	-27.53	152.92
19	Mundaring (Watheroo)	-31.98	116.22
20	Canberra	-35.32	149.00
21	Hobart	-42.92	147.32
22	Macq. Isl.	-54.50	159.00
23	Vanimo	-02.70	141.30
24	Port Morseby	-09.40	147.30
25	Cocos Isl.	-12.20	96.80
26	Hyderabad	17.35	78.47
27	Thumba	8.60	76.90
28	Mirny	-66.50	93.00
29	Sverdlovsk	56.43	58.57
30	Tixie Bay	71.69	128.90
31	Tikhaya	80.60	58.00
32	Tomsk	56.50	84.90
33	Salekhard	66.50	66.50
34	Chita	52.00	113.50
35	Yakutsk	62.00	129.60
36	Ashkhabad	37.90	58.10
37	Alma Ata	43.25	76.92
38	Irkutsk	52.50	104.00
39	Dixon	73.50	80.40
40	YuzhoSakhalinsk	47.00	143.00
41	Vostok	-78.40	106.90

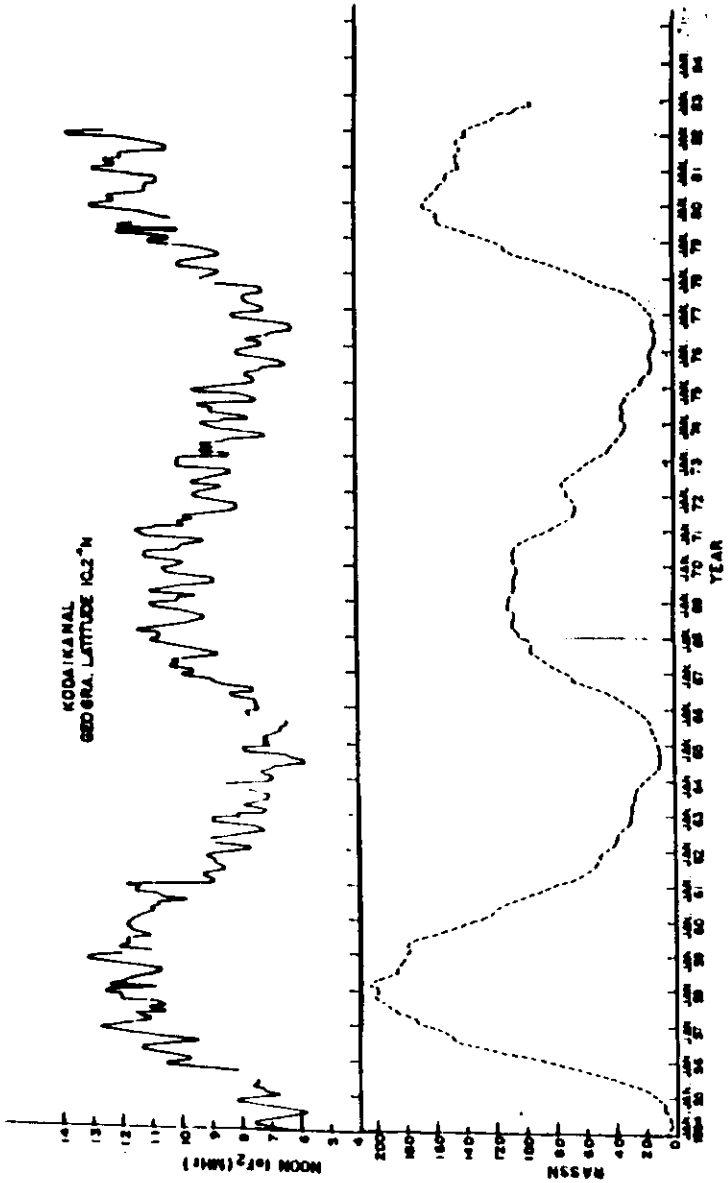

Fig. 1 Sunspot numbers for the three cycles since 1954 (lower part) and noon foF2 values for Kodaikanal. This shows the solar activity variation of the ionosphere.

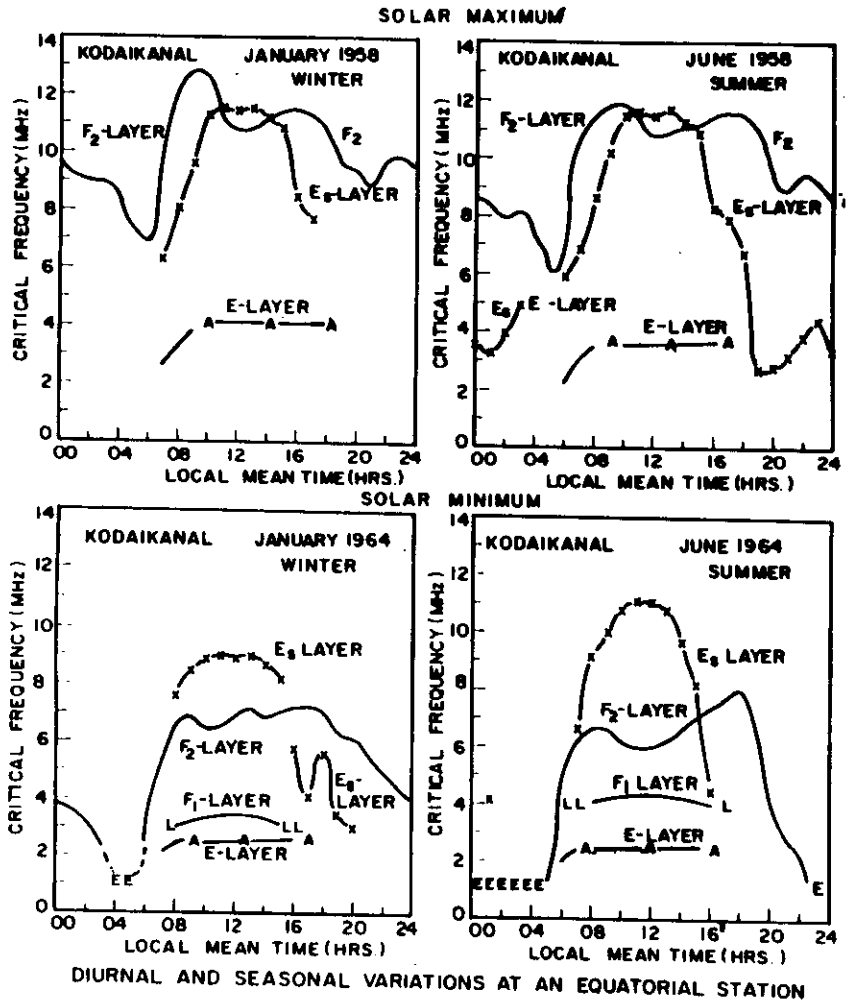

Fig. 2

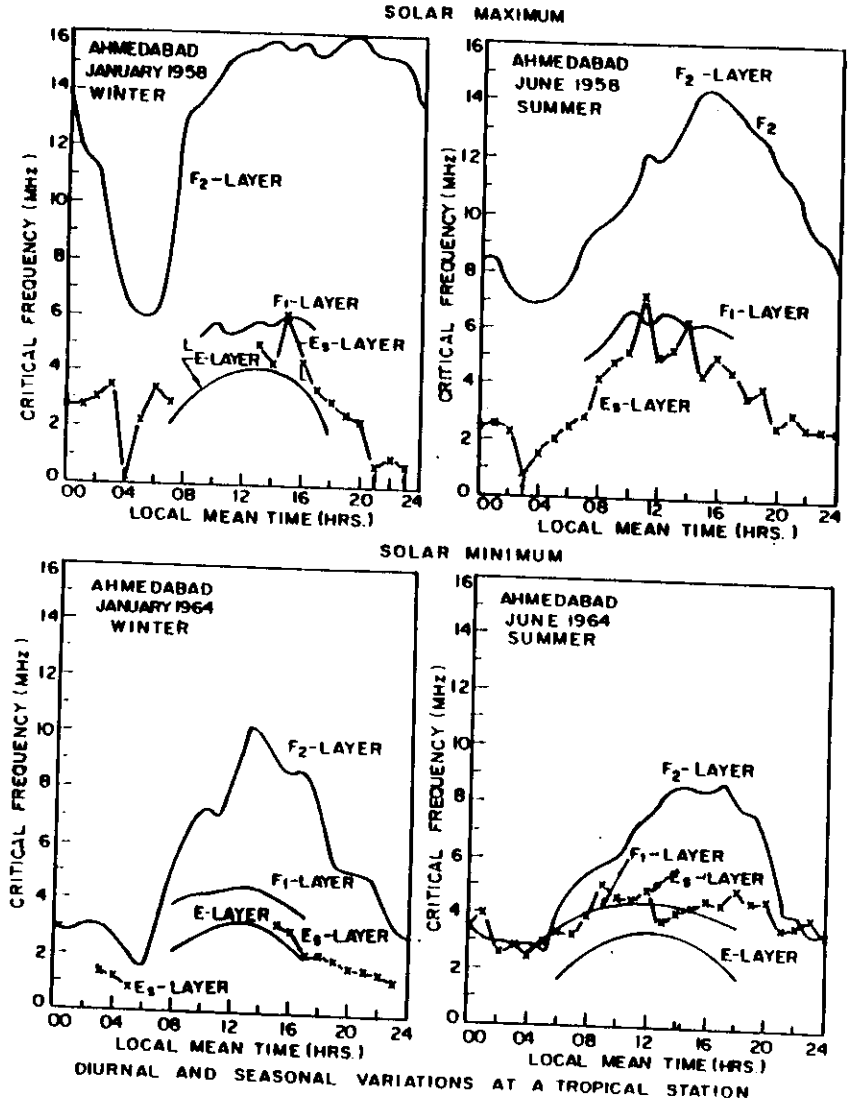

Fig. 3

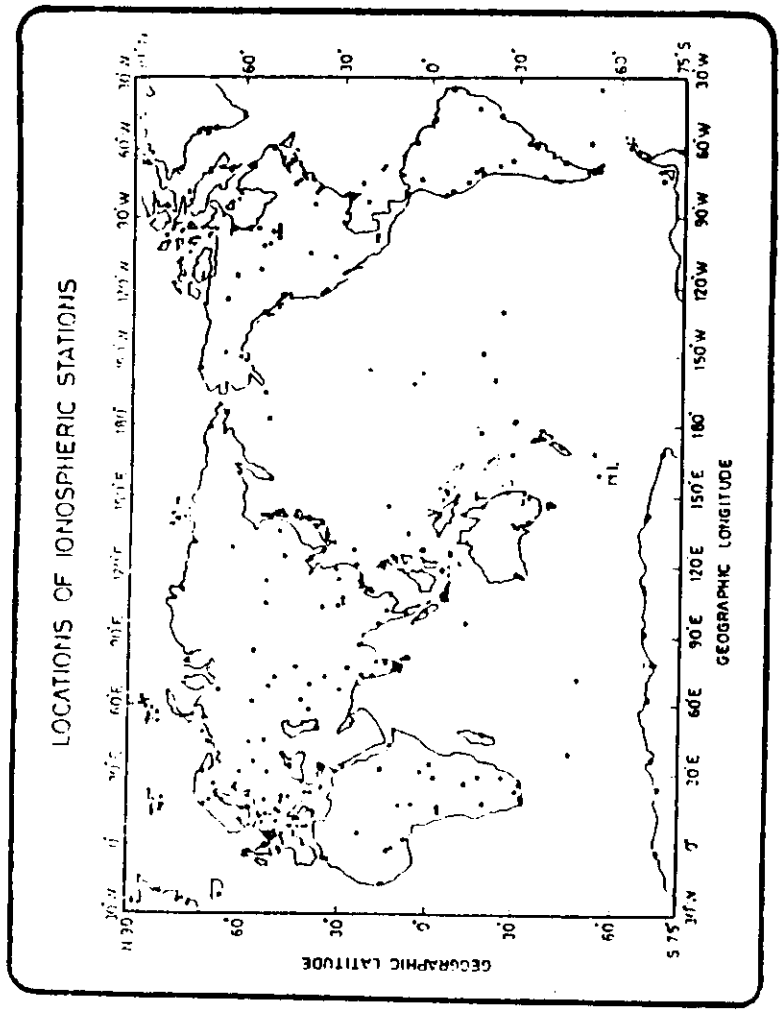

Ionospheric Observation Network

Fig. 4

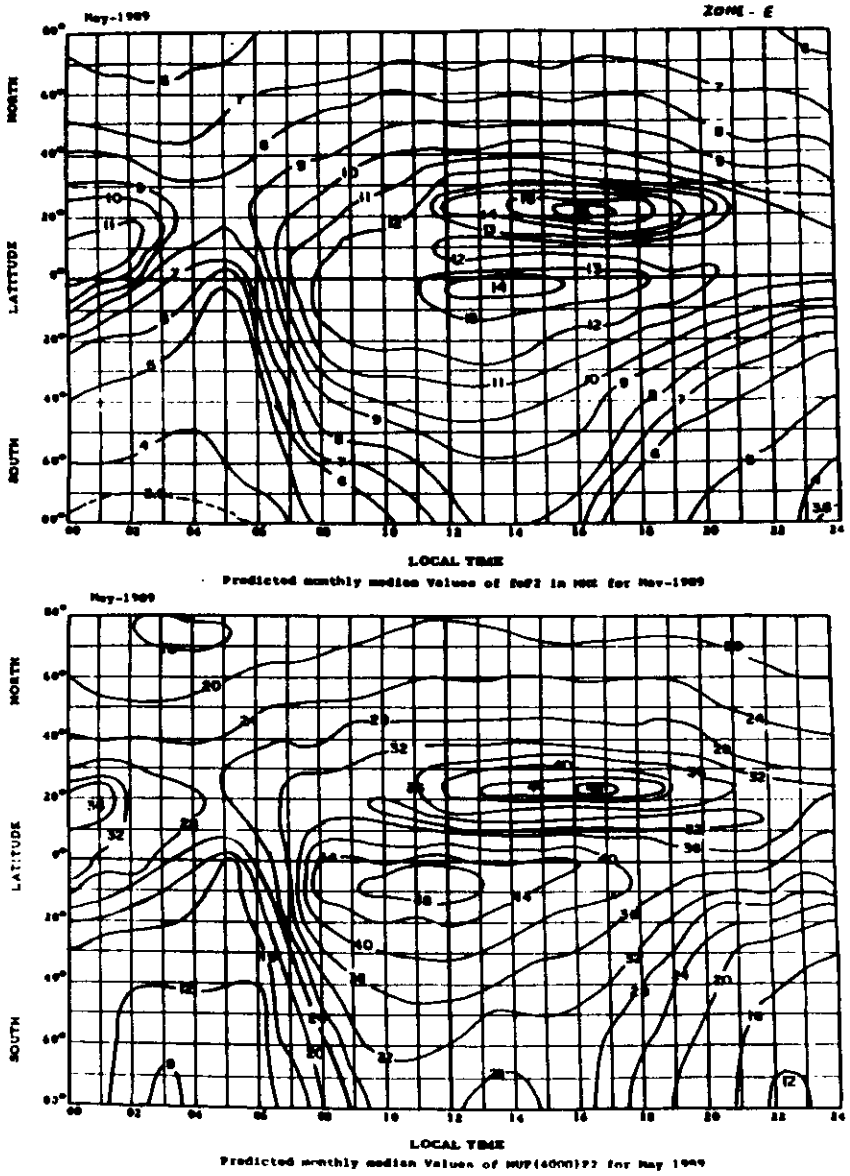

Fig 5

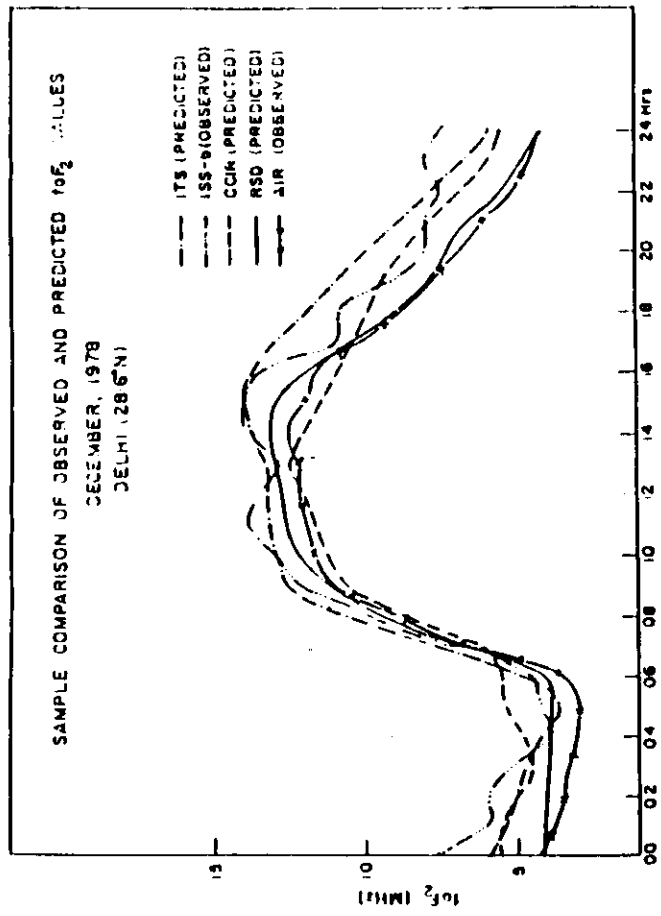

Fig. 6 Comparison of predicted and observed foF2 values by different methods for Delhi. Observed values from ISS-b satellite and AIR ionosonde are also shown in the diagram.

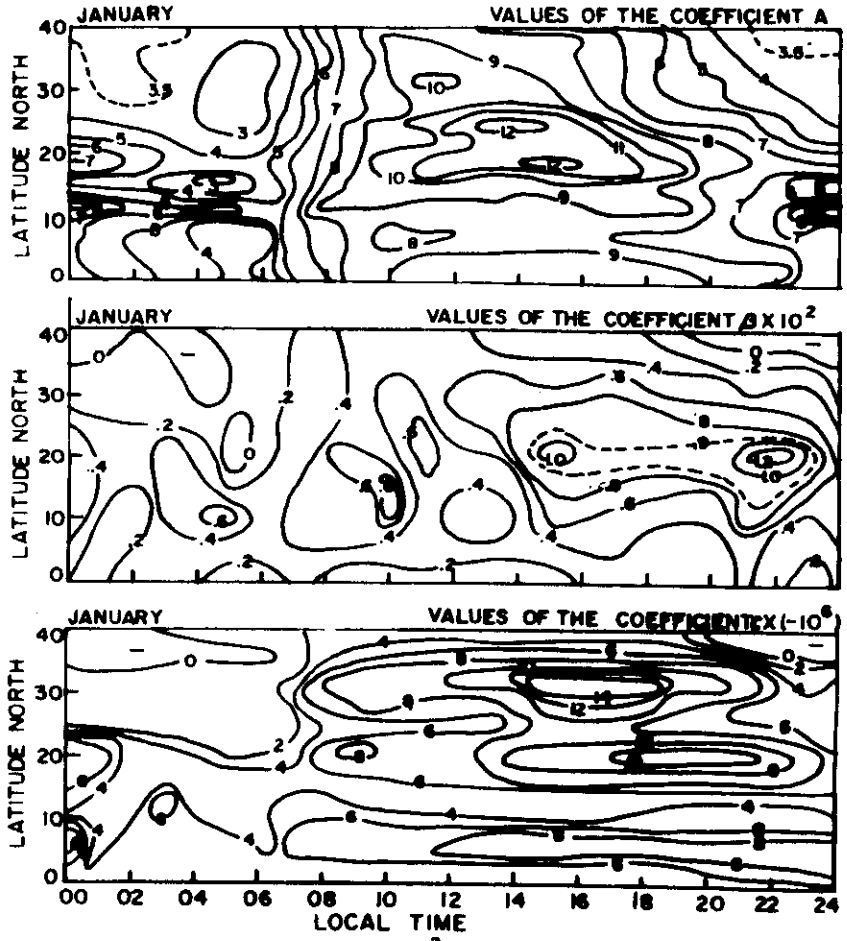

$foF_2 = A + BR + CR^2$ (R = Smoothed Sunspot Number)

Fig. 7

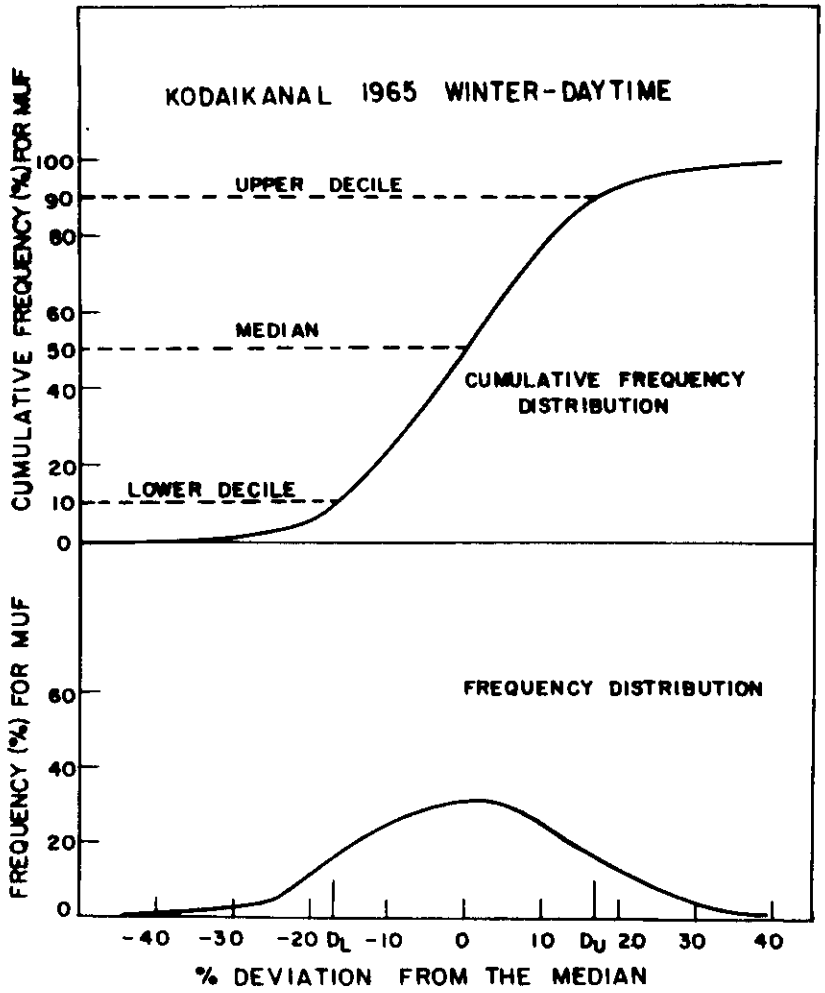

Fig. 8